6-1-2009

Mitogen-activated protein kinase (MAPK) pathways mediate embryonic responses to culture medium osmolarity by regulating Aquaporin 3 and 9 expression and localization, as well as embryonic apoptosis.

Christine E Bell

Nathalie M K Larivière

Patricia H Watson

Andrew J Watson

Human Reproduction, Vol.24, No.6 pp. 1373–1386, 2009
Advanced Access publication on March 3, 2009 doi:10.1093/humrep/dep010

human reproduction

ORIGINAL ARTICLE *Embryology*

Mitogen-activated protein kinase (MAPK) pathways mediate embryonic responses to culture medium osmolarity by regulating Aquaporin 3 and 9 expression and localization, as well as embryonic apoptosis

Christine E. Bell[1,2,3], Nathalie M.K. Larivière[1,2,3,4], Patricia H. Watson[2,4,5], and Andrew J. Watson[1,2,3,4,5,6]

[1]Department of Obstetrics and Gynaecology, The University of Western Ontario, London, Ontario, Canada [2]Department of Physiology and Pharmacology, The University of Western Ontario, London, Ontario, Canada [3]Children's Health Research Institute, London, Ontario, Canada [4]Lawson Health Research Institute, London, Ontario, Canada [5]Department of Medicine, The University of Western Ontario, London, Ontario, Canada

[6]Correspondence address. E-mail: awatson@uwo.ca

BACKGROUND: In order to advance the development of culture conditions and increase the potential for supporting normal preimplantation embryo development *in vitro*, it is critical to define the mechanisms that early embryos utilize to survive in culture. We investigated the mechanisms that embryos employ in response to culture medium osmolarity. We hypothesized that mitogen-activated protein kinase (MAPK) pathways mediate responses to hyperosmotic stress by regulating Aquaporin (AQP) 3 and 9 expression as well as embryonic apoptosis.

METHODS: Real-time reverse transcription and polymerase chain reaction and whole-mount immunofluorescence were used to determine the relative mRNA levels and protein localization patterns of AQP 3 and 9 after hyperosmotic medium treatment.

RESULTS: At 6 and 24 h, a significant increase in *Aqp 3* and *9* mRNA was observed in the sucrose hyperosmotic treatment compared with standard medium and glycerol controls. Blockade of MAPK14/11 negated the increase in *Aqp 3* and *9* mRNA levels, whereas culture in a MAPK8 blocker did not. Hyperosmotic sucrose treatment significantly increased embryonic apoptosis which was negated in the presence of MAPK8 blocker, but not MAPK14/11 blocker.

CONCLUSIONS: MAPK14/11 activation is a component of the rapid adaptive stress response mechanism that includes the effects of AQP mRNA expression and protein localization, whereas the MAPK8 pathway is a regulator of apoptosis.

Key words: programmed cell death / water channels / blastocyst / embryo culture

Introduction

Understanding the interactions between the early embryo and its external environment is critical to developing optimal culture environments for the production of preimplantation embryos and also for understanding the developmental program that controls preimplantation development. Assisted reproductive technologies have long sought to mimic the environment of the reproductive tract to minimize the environmental stress on the preimplantation embryo when cultured *in vitro* (Diamond *et al*., 1991; Leese *et al*., 1998; Kwong *et al*., 2000; Bogdarina *et al*., 2007). Our studies have revealed that up to seven members of the Aquaporin (AQP) gene family are expressed throughout preimplantation development (Offenberg *et al*., 2000) and that AQPs are likely to function in facilitating the *trans*-trophectoderm fluid movements that occur during cavitation which result in the formation of the fluid-filled cavity of the blastocyst (Barcroft *et al*., 2003). AQPs are water channels and represent a family with 13 known members that are expressed in many tissues including

the kidneys, lungs and uterus (Hoffert *et al*., 2000; Offenberg *et al*., 2000; Barcroft *et al*., 2003; Agre, 2006; Hara-Chikuma and Verkman, 2008). AQPs, such as AQP 3 and 9, are aquaglyceroporins and in addition to water, these transmembrane proteins allow the passage of small solutes such as urea and glycerol across the cell membrane (Rivard *et al*., 2005).

More recently, our studies have investigated p38 mitogen-activated kinase (MAPK11/14) pathway expression and function during preimplantation development (Natale *et al*., 2004; Paliga *et al*., 2005; Fong *et al*., 2007; Hickson *et al*., 2007; Madan *et al*., 2007). We have discovered that MAPK11/14 is required to support development beyond the 8–16 cell stage in the mouse and that MAPK11/14 is also activated in response to embryonic exposure to hyperosmotic medium (Natale *et al*., 2004; Paliga *et al*., 2005; Fong *et al*., 2007). Xie *et al*. (2007) reported increased activation of MAPK11/14 and MAPK8 (previously known as the JNK/SAPK pathway) pathways in embryos cultured in poor media compared with those cultured in optimized media. Xie *et al*. (2007) also showed that embryos cultured in less optimal conditions had higher levels of apoptosis than those cultured in optimized media.

Culture medium osmolarity is an important parameter that must be defined to provide embryos with appropriate environments in which to develop *in vitro*. Studies conducted primarily in Dr(s) Baltz's and Gardner's laboratories have demonstrated that *in vivo* reproductive tract environments expose embryos to what would be considered to be hyperosmotic environments for cultured embryos (Gardner and Leese, 1990; Collins and Baltz, 1999). It has been determined that amino acid concentrations, in particular glycine levels, in the oviduct serve as osmolytes to allow for embryo development in 300–350 mOsm environments *in vivo* (Steeves *et al*., 2003; Steeves and Baltz, 2005). *In vitro* preimplantation embryos cultured in >300 mOsm culture medium do not normally progress to the blastocyst stage. However, we have discovered that MAPK11/14 activity is elevated only when embryos are cultured in hyperosmotic sucrose medium and not in hyperosmotic glycerol medium (Fong *et al*., 2007). We propose that exposure to hyperosmotic conditions would increase the ionic gradient across the plasma membrane and this may provide a stimulus for enhanced expression of AQPs in an attempt to alleviate osmotic stress. Since the AQPs expressed during preimplantation development include the aquaglyceroporins AQP 3 and 9, we have investigated the influences of exposure to hyperosmotic culture medium on AQP mRNA levels and protein distribution using either sucrose or glycerol to produce hyperosmotic media. Embryos, and somatic cells in general, do not have the ability to transport sucrose across the plasma membrane, however, the existence of aquaglyceroporins provides early embryos and somatic cells with an avenue for moving glycerol across the plasma membrane. In addition, we have investigated the influences of exposure to hyperosmotic medium on blastocyst apoptosis and characterized the role of MAPK11/14 and the MAPK8 pathways in mediating the responses to hyperosmotic culture media. The early mouse embryo provides an ideal model to investigate the effects of environment on the regulation of AQP expression and function. This cellular model affords an opportunity to define the signaling pathways controlling AQP expression and function. Our results indicate that AQPs are important mediators of embryonic adaptive cellular responses to hyperosmotic stress. We have determined that AQP expression and localization is primarily regulated by the MAPK14/11 pathway, whereas apoptosis is primarily controlled by the MAPK8 pathway.

Materials and Methods

Ovulation induction and mouse embryo collection

Female MF-1 mice (Charles River, Canada; 3–5 weeks old) were injected with 5 IU PMSG (Intervet Canada Ltd, Whitby, Ontario, Canada), followed by 5 IU hCG (Intervet) 47 h later and mated with CD-1 males. Successful mating was determined the following morning (Day 1) by the detection of a vaginal plug. Time post-hCG was used to measure the developmental age of the embryos. Preimplantation mouse embryos were flushed from the reproductive tract using M2 flushing media (Sigma, St Louis, MO, USA) at 65–68 h (8-cell and compacting 8-cell) post-hCG. Embryos were then washed four to five times in 50 μl drops of potassium simplex optimized medium with amino acids (KSOMaa, Chemicon, Temecula, CA, USA) and transferred to 20 μl drops of KSOMaa (Jones *et al*., 1997) or hyperosmotic treatment media, under light paraffin oil. They were maintained in culture under 5% CO_2 in air atmosphere at 37°C for 3, 6 or 24 h. Animal care and treatment followed protocols established by the UWO animal care committee.

Hyperosmotic media

Hyperosmotic media were prepared by the addition of sucrose or glycerol to KSOMaa medium. The treatment groups consisted of (i) KSOMaa (control, 265 mOsm); (ii) KSOMaa + 0.023 g/ml sucrose (300 mOsm); (iii) KSOMaa + 0.032 g/ml sucrose (350 mOsm); (iv) KSOMaa (1 ml) + 0.3 μl (1.26 g/ml) glycerol (300 mOsm) and (v) KSOMaa (1 ml) + 0.7 μl (1.26 g/ml) glycerol (350 mOsm). The osmolarity of the embryo culture medium was tested by freezing-point depression using an Advanced® Model 3320 MicroOsmometer (Advanced Instruments Inc., Norwood, MA, USA).

MAPK14/11 and MAPK8 inhibition

SP600125, MAPK8 inhibitor negative control inactive analog, SB220025 and SB202474 were purchased from Calbiochem (La Jolla, CA, USA). All compounds were dissolved in dimethylsulfoxide (DMSO) to make stock concentrations of 10 mM and were stored at −20°C. Pools of 20 embryos were cultured for 6 or 24 h in 20 μl drops of either (i) KSOMaa plus 0.1% DMSO; (ii) KSOMaa plus 2–10 μM SB220025 (CSAID, active MAPK14/11 inhibitor); (iii) 300 mOsm sucrose hypereosmotic media plus 2–10 μM SB220025; (iv) 350 mOsm sucrose hypereosmotic media plus 2–10 μM SB220025; (v) KSOMaa plus 10 μM SB202474 (CSAID, inactive analog) (Natale *et al*., 2004; Paliga *et al*., 2005; Fong *et al*., 2007); (vi) KSOMaa plus 10 μM SP600125 (active MAPK8 inhibitor) (Xie *et al*., 2006) or (vii) 300 mOsm sucrose hypereosmotic media plus 10 μM SP600125; (viii) 350 mOsm sucrose hypereosmotic media plus 10 μM SP600125; (ix) KSOMaa plus 10 μM MAPK8 inhibitor negative control inactive analog (CSAID, MAPK8 negative control inactive analog).

RNA extraction

Total RNA was extracted from the pools of 20 embryos or from positive control tissue (mouse heart, liver and kidney; 1 μg). Samples were frozen and stored at −80°C in 5 μl of lysis buffer and processed as outlined in a Microeasy RNA isolation Kit protocol (Qiagen, Mississauga, Ontario, Canada) following collection. In samples used for real-time reverse transcription and polymerase chain reaction (RT–PCR) analysis, 0.025 pg/embryo of exogenous Luciferase control RNA (Promega Corporation,

Madison, WI, USA) containing a 30-base poly(A) tail was added to each pool of embryos prior to RNA extraction.

Reverse transcription and polymerase chain reaction

Embryo total RNA was reverse transcribed (RT) using Random Primers (Invitrogen Life Technologies, Burlington, ON, Canada) and RNaseOUT™ Ribonuclease Inhibitor (Invitrogen Life Technologies) along with Sensiscript RT (Qiagen) according to the manufacturer's suggested protocol. Following 1 h incubation, the sample was diluted to a concentration of one embryo equivalent per microliter (embryo/μl) and subjected to PCR amplification of *Luciferase*, to determine the efficiency of the RNA extraction and reverse transcription prior to investigation of expression of the target genes by real-time PCR amplification.

Custom TaqMan® gene expression assay design for real-time PCR

The Custom TaqMan® primer and probe sets for *Luciferase* were designed using the Assays-by-Design File Builder program (Applied Biosystems, Foster City, CA, USA). The probe sequence for luciferase was directed against a target site 550 bp into the full-length sequence used to generate the Luciferase Control RNA (Promega Corporation). The target site specifies an approximate location for the generation of a TaqMan® probe, and each target site was verified to be unique by performing the BLAST® analysis. Dual-labeled probes were synthesized (Applied Biosystems) to contain the reporter dye 6-carboxyfluorescein (6-FAM) at the 5′ end and a non-fluorescent quencher dye at the 3′ end.

Real-time RT–PCR analysis

Real-time RT–PCRs were performed using the ABI PRISM® 7900HT sequence detection system (Applied Biosystems) and TaqMan® gene expression assays (Applied Biosystems). Pre-designed and pre-optimized commercially available TaqMan® gene expression assays for *Aqp 3* (Assay ID: mm01208559_m1), *9* (Assay ID: mm00508094_m1), were used along with the Custom TaqMan® gene expression assays described above for *Luciferase*. The PCR mixture (50 μl) contained 25 μl of TaqMan® Universal PCR Master Mix (2× concentration, containing AmpliTaq Gold® DNA Polymerase, AmpErase® UNG, dNTPs with dUTP, Passive Reference 1 and optimized buffer components; Applied Biosystems), 2.5 μl of the appropriate 20× TaqMan® gene expression assay (see above), 10 μl of embryo cDNA (at a diluted concentration of 0.1 embryo/μl) corresponding to one embryo equivalent per reaction and 12.5 μl of HyPure™ Molecular Biology Grade Water (HyClone, Logan, UT, USA). Thermal cycling conditions were 50°C for 2 min and 95°C for 5 min, followed by up to 60 cycles of 95°C for 15 s, and a combined annealing extension stage, 60°C for 1 min. Each reaction was performed in triplicate on ABI PRISM® 96-well optical reaction plates (Applied Biosystems). Relative quantification of target gene expression levels was performed using the comparative C_T (threshold cycle) method (ABI PRISM® sequence detection system, version 2.1, Applied Biosystems). The quantification was normalized to the control luciferase RNA levels (Li *et al*., 2005). Within the log linear phase region of the amplification curve, the difference between each cycle was equivalent to a doubling of the amplified product of the PCR. The ΔC_T value was determined by subtracting the control C_T value for each sample from the target gene C_T value of the sample. Calculation of $\Delta\Delta C_T$ used KSOMaa control treatment as the standard for determining fold-changes in the relative mRNA expression of the target gene using the formula $2^{-\Delta\Delta C_T}$.

Antisera

Immunolocalization of AQP 3 and 9 in treated 8-cell embryos was determined by using proven commercially available primary antibodies from Alpha Diagnostic Int. (San Antonio, TX, USA) consisting of: (i) rabbit polyclonal anti-rat AQP 3, directed against a 15-amino-acid sequence from the C terminus of rat AQP 3 and (ii) rabbit polyclonal anti-rat AQP 9, raised against a 19-amino-acid synthetic peptide from the rat AQP 9 C-terminal domain. The antisera were employed at a dilution of 1:100 in combination with a goat anti-rabbit whole IgG secondary antibody (Jackson ImmunoResearch, West Grove, PA, USA). Each antibody has been extensively characterized in western blot and immunolocalization studies on mouse and rat tissues, and established as specific for their target proteins (Ishibashi *et al*., 1994; Ma *et al*., 1994; Ecelbarger *et al*., 1995; Echevarria *et al*., 1996; Ishibashi *et al*., 1997; Koyama *et al*., 1997; Ishibashi *et al*., 1998; Barcroft *et al*., 2004).

Indirect immunofluorescence detection of AQP 3 and 9

Mouse embryos were collected from the reproductive tracts of superovulated female MF-1 mice as described above. Embryo pools were washed in 1× PBS (GIBCO) and fixed for indirect immunofluorescence in 2% paraformaldehyde in PBS at room temperature for 30 min. Fixed embryos were washed once in 1× PBS and either used immediately or stored at 4°C in embryo storage buffer (1× PBS + 0.9% sodium azide) for up to 1 week before processing for whole-mount indirect immunofluorescence as previously described (Jones *et al*., 1997; Betts *et al*., 1998; MacPhee *et al*., 2000; Barcroft *et al*., 2003, 2004). Fixed embryos were permeabilized in blocking buffer (0.01% Triton X-100 + 5% normal goat serum in 1× PBS) at room temperature for 30 min followed by two washes in fresh PBS. Embryos were incubated with primary antibody for AQP 3 or 9 at a 1:100 dilution in antibody dilution/wash buffer (ADB; 0.005% Triton X-100 + 1% normal goat serum in 1× PBS) at 4°C overnight. Negative controls included embryos incubated in ADB alone without the addition of the primary antibody in order to determine the levels of non-specific fluorescence. Embryos were then washed three times for 20 min in ADB at 37°C and incubated with fluorescein isothiocyanate (FITC)-conjugated secondary antibody (1:200 in ADB) at 4°C overnight, followed by three washes for 20 min in ADB at 37°C. Fully processed embryos were mounted onto glass slides in 20 μl of FluoroGuard anti-fade reagent (BioRad) under elevated 22 × 22 mm glass coverslips (No. 1 thickness), and slide preparations were sealed with nail polish. Slides were stored for up to 2 days at 4°C in a light tight box prior to immunofluorescence imaging employing a BioRad MRC600 Confocal Laser Scanning Microscope. In total, 20–30 embryos for each treatment were examined for each of the two primary antisera.

Hyperosmotic treatment of embryos for apoptosis assessment

Embryos were collected as described above. They were then placed in KSOMaa or hyperosmotic sucrose or glycerol media, with or without inhibitors, for 6 h. They were then washed in fresh 50 μl KSOMaa drops and placed into fresh 20 μl KSOMaa drops and culture as described above.

TUNEL apoptosis assay

Cleavage of genomic DNA during apoptosis yields single strand breaks in high molecular weight DNA, which can be identified by labeling the free 3′-OH terminal with modified nucleotides in an enzymatic reaction (Saraste and Pulkki, 2000; Huerta *et al*., 2007). Once the blastocyst stage was reached, embryo pools were fixed for 1 h in 2%

paraformaldehyde in PBS and washed in PBS. Fixed embryos were then permeabilized and blocked by room temperature incubation for 1 h in permeabilization solution (1% sodium citrate + 0.01% Triton X-100). The first negative controls did not undergo permeabilization. The embryos were then placed into a humidified chamber and put into a 4°C fridge for 2 min. They were then washed again in PBS, and a positive control group was removed from the treatment groups and treated with 100 μl DNAse solution (10 μl DNAse1 in 990 μl 50 mM Tris-HCl) for 10 min at room temperature. This was done to induce strand breaks, allowing for the assessment of maximal DNA fragmentation during analysis. A second group of embryos was removed from the treatment groups to serve as the second negative control for fixed embryos. Both groups of negative control embryos were put into 50 μl TUNEL label solution (nucleotide mixture in reaction buffer). The positive control and the treatment groups were placed in 50 μl TUNEL reaction mixture (terminal deoxynucleotidyl transferase from calf thymus, recombinant in *Escherichia coli*, in storage buffer + nucleotide mixture in reaction buffer). The TUNEL reaction mixture-labeled DNA strand breaks through terminal deoxynucleotidyl transferase, which catalyzes polymerization of labeled nucleotides to the free 3′-OH DNA ends in a template-independent manner, and by incorporating fluorescein labels in nucleotide polymers (Byrne *et al*., 1999; Saraste and Pulkki, 2000). The fluorescein label was detected by epifluorescence microscopy. The two negative controls, the positive control and the treatment groups were incubated for 60 min in a humidified chamber at 37°C. Upon removal from the chamber, the groups were washed in 0.5 μl DAPI (4',6-diamidino-2-phenylindole dihydrochloride; Sigma-Aldrich; diluted 1:2000 from 1 mg/ml stock solution) + 200 μl PBS for 30 min, to stain the DNA within the nuclei. The groups were washed twice more in 200 μl PBS, leaving 15 min between the washes. Fully processed embryos were mounted onto glass slides in a drop of FluoroGuard™ anti-fade reagent (BioRad Laboratories Canada Ltd., Mississauga, ON, Canada). Fluorescence imaging was conducted on a Zeiss Axiovert 100 inverted microscope equipped with epifluorescence optics and digital image analysis software (Carl Zeiss Inc., Thornwood, NY, USA).

Caspase-3 assay for apoptosis

Activated caspase-3 in preimplantation embryos was detected using the PhiPhilux G1D2 kit (OncoImmunin Inc., College Park, MD, USA). Briefly, embryos serving as the positive control were removed from the treatment groups and treated with 100 μl DNAse solution (10 μl DNAse1 in 990 μl 50 mM Tris-HCl) for 10 min at room temperature. Following this, 10–15 embryos from each treatment were incubated with 30 μl caspase-3 substrate under oil for 1 h at 37°C in air with 5% CO_2. After three washes in dilution buffer, embryos were fixed with 2% paraformaldehyde in PBS for 30 min at 4°C in the dark. After three washes in PBS, the first of which contained DAPI, fully processed embryos were mounted onto glass slides in a drop of FluoroGuard™ anti-fade reagent (BioRad). Fluorescence imaging was conducted on a Zeiss Axiovert 100 inverted microscope equipped with epifluorescence optics and digital image analysis software (Carl Zeiss Inc.).

Apoptotic fluorescence image analysis

Apoptotic fluorescence was assessed by first counting the number of DAPI-stained (blue) nuclei, visualized by an excitation wavelength of 450–500 nm, representing the total number of cells in the early embryo. Then, the FITC-stained (green) apoptotic nuclei were counted, visualized by an excitation wavelength of 515–565 nm. To obtain the percent of apoptotic cells, the number of FITC-stained cells was divided by the DAPI-stained cells. All microscope and image capture settings remained constant during the digital capture of micrographs between embryos and between treatment groups. Acquired micrographs were saved in TIFF image format and processed using Adobe Photoshop CS2 (Adobe Systems Inc., San Jose, CA, USA) for recognition, selection and separation of the desired chromogen signal. Qualitative analysis was done by separation of the blue channels (representing DAPI-stained nuclei) and the green channels (representing FITC fluorescence of fragmented DNA).

Statistical analysis

Statistical analysis of data was carried out using SPSS®, version 12.0 (SPSS Inc., Chicago, IL, USA) software package. TUNEL assay and caspase-3 assay results are presented as the mean ± SEM for percent apoptosis from three independent replicates. All data were tested for homogeneity of variances by independent sample *t*-tests for equality of variances. In instances of equal variance, data were subjected to one-way analysis of variance (ANOVA), and followed by Tukey's multiple comparison test. When equal variances were not observed, data were arcsine-transformed and then subjected to ANOVA, followed by Tukey's multiple comparison test. For all data analysis, $P \leq 0.05$ was considered statistically significant.

Results

Experimental design

Our first objective was to define the experimental parameters. Eight-cell mouse embryos were cultured in normal KSOMaa (265 mOsm), and KSOMaa made hyperosmotic with either sucrose or glycerol to 300 and 350 mOsm. Embryos were cultured for 3, 6 and 24 h and examined and fixed or frozen for immunofluorescence or real-time RT–PCR. Figure 1 shows representative phase contrast images of embryos cultured under the above described conditions. Embryos cultured in KSOMaa for 24 h progressed normally to the blastocyst stage. Embryos cultured in 300 mOsm sucrose medium compacted, but were unable to progress to the blastocyst stage. Embryos cultured in 350 mOsm sucrose medium were delayed developmentally and did not compact or proceed to the blastocyst stage. In contrast, embryos cultured in glycerol hyperosmotic media at both 300 and 350 mOsm compacted and progressed normally to the blastocyst stage (Fig. 1).

Aqp 3 mRNA levels after hyperosmotic treatment using sucrose or glycerol

There was no significant difference in *Aqp 3* mRNA abundance after 3 h in hyperosmotic media (data not shown). *Aqp 3* expression after 6 h (Fig. 2A) in 350 mOsm sucrose media was significantly elevated undergoing a 2.14-fold increase over KSOMaa control mRNA levels. After 24 h, *Aqp 3* (Fig. 2B) mRNA levels were significantly elevated by 2.64-fold in 300 mOsm sucrose over control levels, but were not significantly elevated in embryos cultured in 350 mOsm sucrose. Interestingly, after 6 and 24 h in glycerol treatment, *Aqp 3* mRNA levels were significantly decreased ($P \leq 0.05$) in embryos cultured in 350 mOsm glycerol medium (Fig. 2C and D). *Aqp 3* mRNA levels were decreased by 80% compared with KSOMaa control levels after 6 h and 60% from KSOMaa control levels after 24 h in 350 mOsm glycerol hyperosmotic treatment.

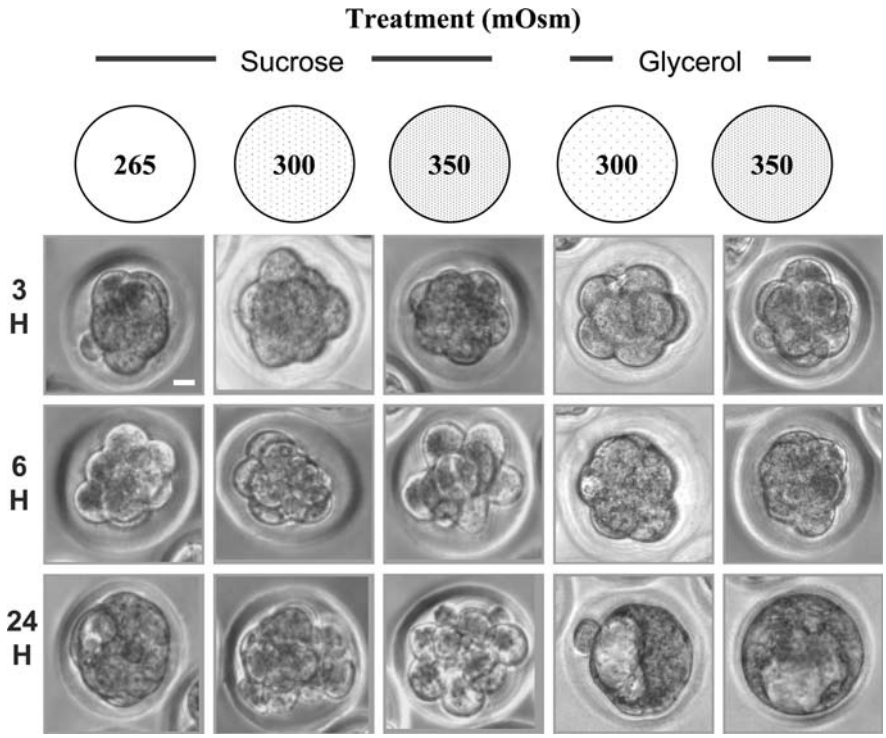

Figure 1 Phase contrast images of embryos cultured in hyperosmotic media using sucrose or glycerol. Phase contrast images of embryos cultured in 265 (normal KSOMaa), 300 (KSOMaa + sucrose or glycerol) or 350 mOsm (KSOMaa + sucrose or glycerol). Embryos were cultured for 3, 6 or 24 h before development was assessed based on morphology. Embryos cultured in KSOMaa, KSOMaa + 300 mOsm glycerol and KSOMaa + 350 mOsm glycerol were all able to develop to the blastocyst stage in normal proportions. Embryos cultured in 300 mOsm sucrose compacted, but did not cavitate. Embryos cultured in 350 mOsm did not compact and arrested at the 8–16 cell stage; Scale bar = 20 μM.

Aqp 9 mRNA levels after hyperosmotic treatment using sucrose or glycerol

There was no significant difference in *Aqp 9* mRNA abundance after 3 h in hyperosmotic media (data not shown). *Aqp 9* mRNA expression underwent a 1.97-fold increase after 6 h (Fig. 2E) in 300 mOsm sucrose media over KSOMaa control levels and a 2.73-fold increase in 350 mOsm sucrose media over control levels. By 24 h, *Aqp 9* mRNA expression was significantly ($P \leq 0.05$) increased by 4.3-fold in 300 mOsm sucrose and 8-fold in 350 mOsm sucrose over control levels (Fig. 2F). Figure 2G and H indicate that in contrast to the sucrose hyperosmotic treatment results, *Aqp 9* mRNA levels were not significantly increased in any of the glycerol medium treatment groups at either time point.

AQP 3 and 9 protein localization after hyperosmotic treatment using sucrose or glycerol

AQP protein localization was next investigated using whole-mount immunofluorescence for AQP 3 and 9 polypeptides. Figure 3 displays representative images of normal distribution of AQP 3 (Fig. 3A and D) and 9 (Fig. 3G and J) and abnormal distribution of AQP 3 and 9 after exposure to hyperosmotic conditions. These images represent the range of morphologies observed after exposure to hyperosmotic media. There were no visible changes in AQP 3 or 9 localization after 3 h in hyperosmotic media (data not shown). Both polypeptides maintained the cortical, apolar localization patterns reported by Barcroft *et al.* (2003). After 6 h, however, AQP 3 localization shifted from the cortical distribution to become primarily cytoplasmic under 300 and 350 mOsm sucrose medium conditions (Fig. 3B and C). After 24 h in sucrose hyperosmotic media, the AQP 3 distribution became predominantly cytoplasmic (Fig. 3E and F). Localization of AQP 9 underwent a more dramatic change to become predominantly cytoplasmic in both 300 and 350 mOsm sucrose medium treatments at 6 h, although some cortical localization was observed (Fig. 3H and I). AQP 9 distribution remained cytoplasmic in both 300 and 350 mOsm at 24 h, although some cortical expression was observed (Fig. 3K and L). AQP 3 and 9 protein localization was not affected by culture in glycerol medium in any of the treatment groups or at any time point (data not shown).

Aqp 3 and 9 mRNA levels after hyperosmotic treatment using sucrose in the presence of a MAPK14/11 inhibitor

Our next objective was to define the signaling pathways regulating the sucrose hyperosmotic treatment induction of AQP mRNA expression. We first examined the effects of blocking MAPK14/11 on *Aqp* mRNA levels. To address this, embryos were cultured in sucrose hyperosmotic media as described above with the addition of 2 μM SB220025

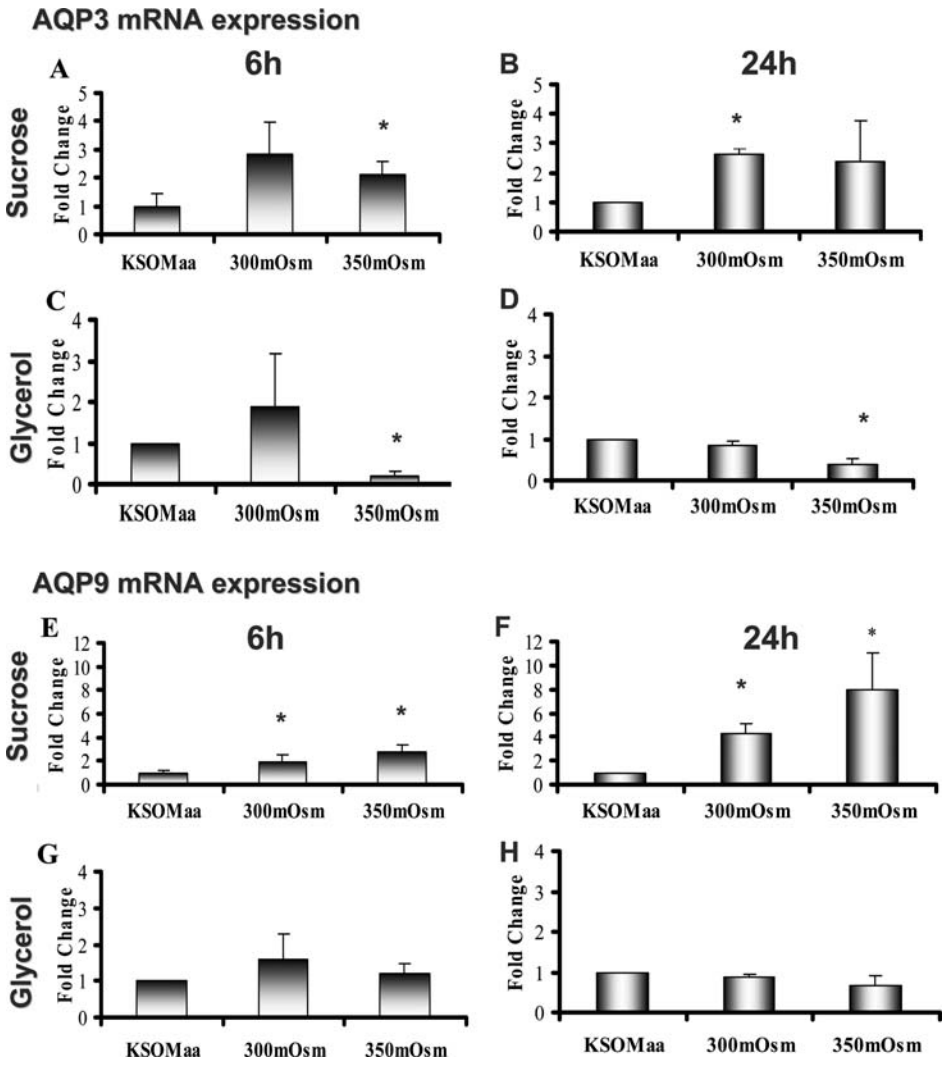

Figure 2 Relative *Aqp 3* and *9* mRNA levels following treatment. Real-time RT–PCR was used to determine the relative mRNA levels of *Aqp 3* after 6 (**A**) or 24 h (**B**) in sucrose hyperosmotic media. *Aqp 3* mRNA was significantly elevated after (A) 6 h in 350 mOsm and (B) 24 h in 300 mOsm; $n = 3$, mean $\pm$ SE, $P \leq 0.05$. Real-time RT–PCR was used to determine the relative mRNA levels of *Aqp 3* following (**C**) 6 or (**D**) 24 h exposure to glycerol hyperosmotic medium treatment. There were no significant increases in *Aqp 3* mRNA levels between glycerol medium treatments and KSOMaa (265 mOsm) control. Real-time RT–PCR was used to determine the relative mRNA levels of *Aqp 9* after 6 (**E**) or 24 h (**F**) in sucrose hyperosmotic media. *Aqp 9* mRNA was significantly elevated in embryos cultured for (E) 6 and (F) 24 h in 300 and 350 mOsm treatment media. In contrast, treatment for (**G**) 6 and (**H**) 24 h exposure to glycerol hyperosmotic medium did not result in a significant change in mRNA levels for *Aqp 9* between glycerol medium treatments and KSOMaa (265 mOsm) (G,H).

(Natale *et al.*, 2004). The 3 h time point was not included (nor the glycerol treatments) in these experiments because *Aqp 3* and *9* mRNA expression did not vary from controls under these conditions. In contrast to what was observed with sucrose hyperosmotic media alone (Fig. 2A), after 6 h of treatment with sucrose media in the presence of MAPK14/11 inhibitor, we did not detect a significant increase in *Aqp 3* mRNA levels (Fig. 4A) compared with KSOMaa control levels. However, after 24 h, we observed a significant decrease in the *Aqp 3* mRNA levels (Fig. 4B). In contrast to what was observed with sucrose hyperosmotic media alone, in the presence of the MAPK11/14 inhibitor, *Aqp 9* mRNA levels did not significantly increase in sucrose media after 6 (Fig. 4E) or 24 h (Fig. 4F) compared with KSOMaa control levels. AQP 3 and 9 protein localization following sucrose hyperosmotic treatment and MAPK14/11 inhibitor did not vary from that observed in untreated controls, indicating that MAPK14/11 blockade negated the transition to a predominantly cytoplasmic distribution observed following sucrose hyperosmotic medium treatment (data not shown).

Aqp 3 and 9 mRNA levels after hyperosmotic treatment using sucrose in the presence of a MAPK8 inhibitor

We next investigated whether the MAPK8 pathway may also regulate *Aqp 3* and *9* mRNAs following exposure to hyperosmotic media. To address this, embryos were cultured in sucrose hyperosmotic

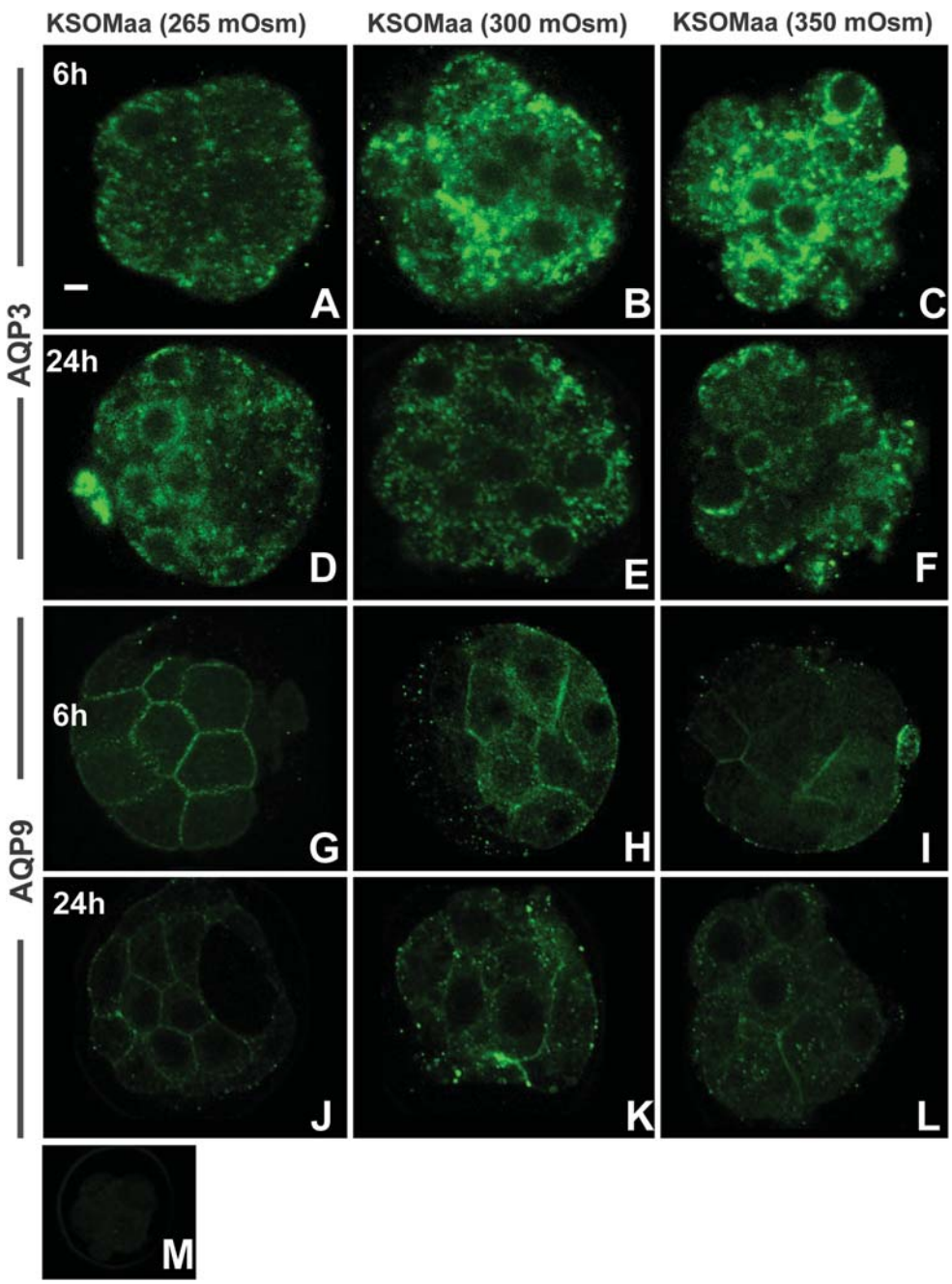

Figure 3 AQP 3 and 9 protein localization following treatment with sucrose or glycerol hyperosmotic medium. Representative images of AQP 3 after 6 (**A**–**C**) or 24 h (**D**–**F**) exposure and AQP 9 after 6 (**G**–**I**) or 24 h (**J**–**L**). AQP 3 and 9 protein localization pattern varied by 6 (B,C; H,I) and 24 h (E,F; K,L) in sucrose hyperosmotic medium from normal distribution patterns in KSOMaa (A,D; G,J), showing enhanced cytoplasmic components of normal AQP 3 and 9 localization. Glycerol treatment did not affect AQP 3 and 9 localization compared with untreated controls. $n = 20–30$ embryos in each group; scale bar = 20 μM. No primary antibody negative control (**M**).

media as described above with the addition of 10 μM SP600125 (Xie *et al*., 2006, 2007). The 3 h time point was not included (nor the glycerol treatments) in these experiments because *Aqp 3* and *9* mRNA expression did not vary from controls under these conditions (see above). After 6 h of treatment with 350 mOsm sucrose hyperosmotic medium in the presence of MAPK8 inhibitor, we still observed significant increases in *Aqp 3* (Fig. 4C) and *9* (Fig. 4G) mRNA levels compared with KSOMaa control levels. After 24 h, we also observed significant increases in *Aqp 3* (Fig. 4D) and *9* (Fig. 4H) mRNA levels in 350 mOsm sucrose hyperosmotic medium compared with the KSOMaa control. In the presence of a MAPK8 inhibitor, AQP 3 and 9 protein distribution predominantly consisted of the expected cortical distribution observed in untreated controls but also included a cytosolic component in the presence of hyperosmotic media and

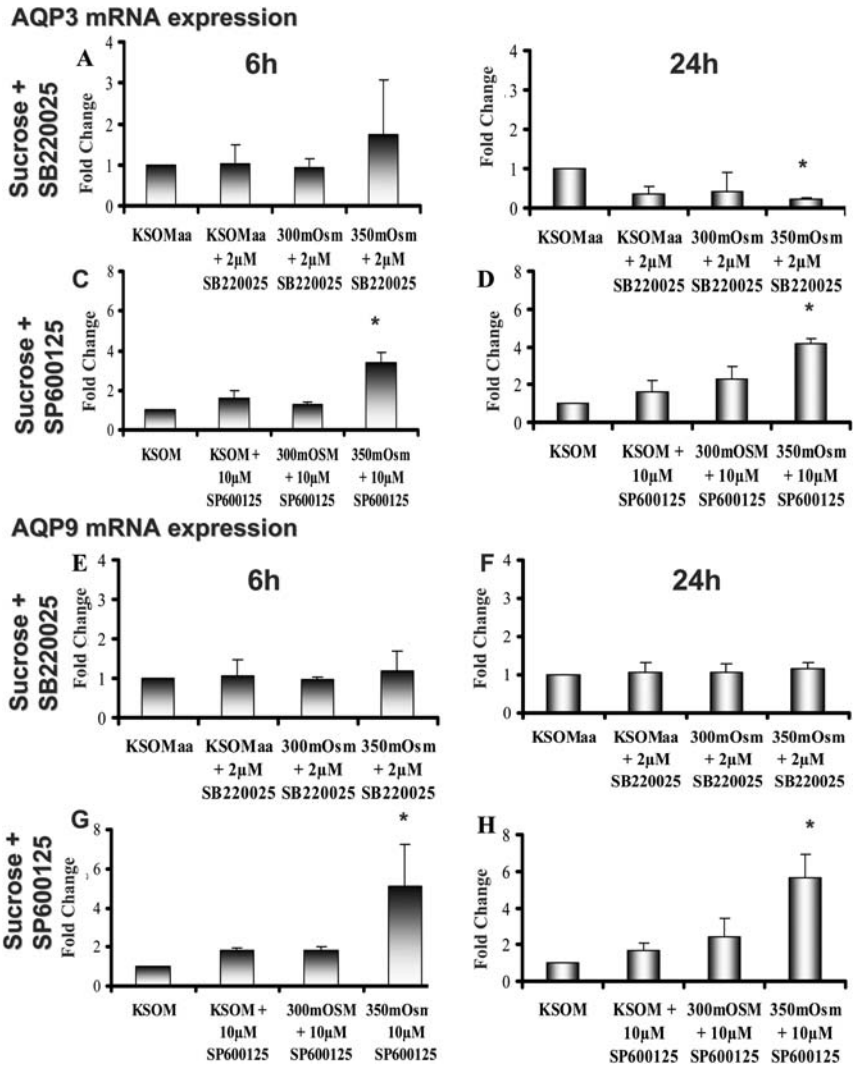

Figure 4 Relative *Aqp 3* and *9* mRNA levels following treatment in the presence of either a MAPK14/11 or MAPK8 inhibitor. Real-time RT–PCR was used to determine the relative mRNA levels of *Aqp 3* after (**A**) 6 or (**B**) 24 h exposure to sucrose hyperosmotic medium treatment + SB220025 (a MAPK14/11 inhibitor). No significant increases in *Aqp 3* mRNA levels were observed after (A) 6 h but after (B) 24 h exposure to sucrose hyperosmotic media Aqp 3 mRNA levels significantly declined in the presence of SB220025. The *Aqp* mRNA levels of *Aqp 9* after (**E**) 6 or (**F**) 24 h exposure to sucrose hyperosmotic medium treatment + SB220025 did not vary significantly between any treatments after (E) 6 or (F) 24 h. The relative mRNA levels of *Aqp 3* were measured after (**C**) 6 or (**D**) 24 h exposure to sucrose hyperosmotic medium treatment + SP600125 (a MAPK8 inhibitor). There was a significant increase in *Aqp 3* mRNA after 6 (C) and 24 h (D) in embryos exposed to 350 mOsm sucrose hyperosmotic medium treatment + SP600125; $n = 3$, mean ± SE, $P \leq 0.05$. The Aqp 9 mRNA levels after (**G**) 6 or (**H**) 24 h exposure to sucrose hyperosmotic medium treatment + SP600125 were significantly increased compared with control values; $n = 3$, mean ± SE, $P \leq 0.05$.

the MAPK8 blocker (data not shown). These data suggest that the MAPK8 pathway is not a primary mediator of the variations in level and expression in AQP 3 and 9 in response to hyperosmotic stress.

Apoptosis in embryos cultured in KSOMaa, 300 and 350 mOsm sucrose or glycerol media

Our results to this point indicate that sucrose hyperosmotic treatment affects AQP mRNA and protein distribution, and these effects are primarily mediated via the MAPK14/11 pathway and not the MAPK8 pathway. We next investigated whether hyperosmotic treatment would affect the incidence of cell death or apoptosis. We hypothesized that the presence of aquaglyceroporins would reduce the incidence of apoptosis in the presence of glycerol hyperosmotic treatment. Eight-cell mouse embryos were treated with the respective medium for 6 h and then placed into normal KSOMaa medium for assessment of apoptosis at the blastocyst stage (24 h in culture total time). Analysis of apoptosis by TUNEL in blastocysts after 6 h in KSOMaa, 300 or 350 mOsm KSOMaa using glycerol or sucrose revealed that there was a significant increase ($P \leq 0.05$) in apoptotic

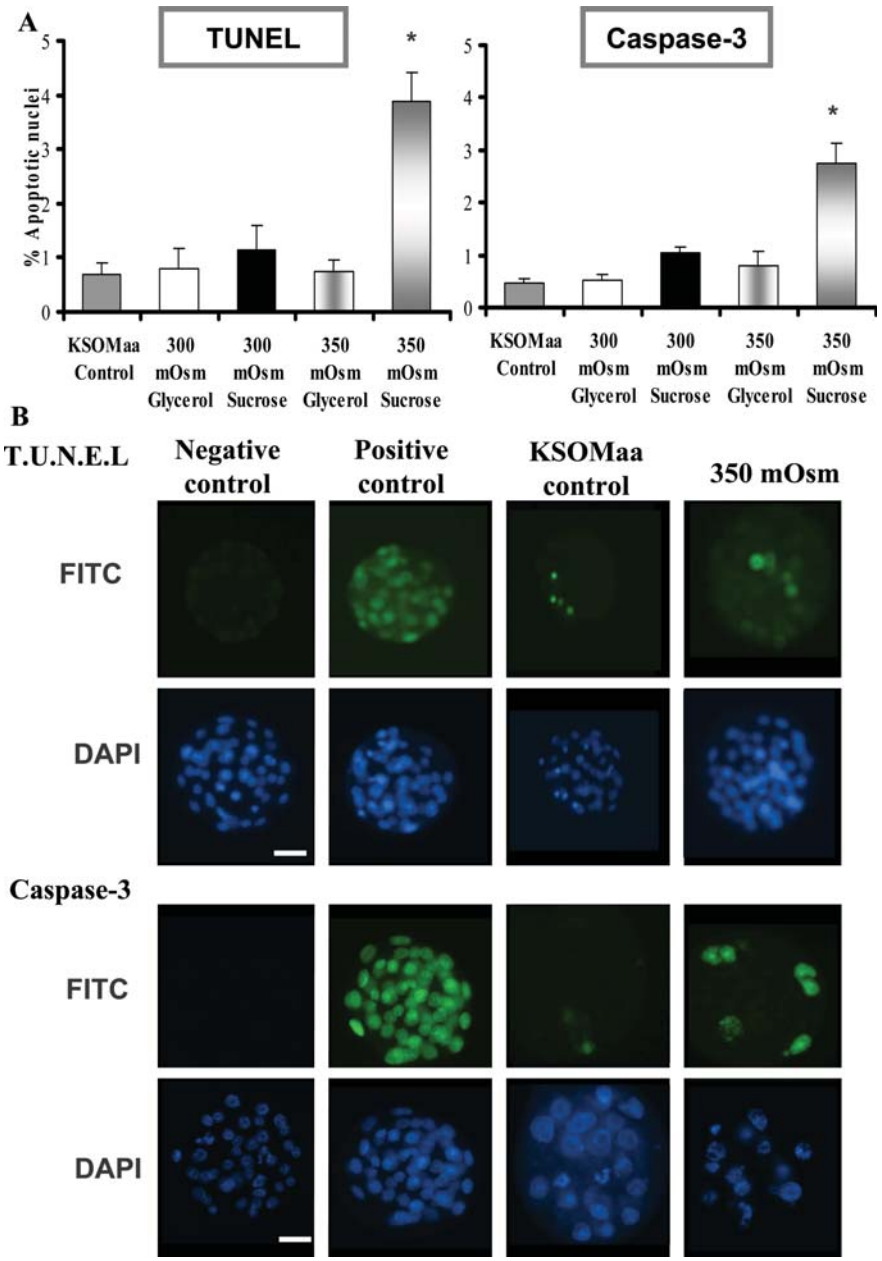

Figure 5 Apoptosis following hyperosmotic media treatment for 6 h. (**A**) TUNEL and caspase-3 assays were used to assess the level of apoptosis in blastocysts after having been exposed to hyperosmotic media for 6 h and then allowed to develop to the blastocyst stage in normal KSOMaa media. Embryos cultured in glycerol hyperosmotic media displayed the same level of apoptosis as control embryos cultured in KSOMaa. Embryos cultured in 350 mOsm sucrose medium displayed a significant increase in apoptosis compared with controls; mean $\pm$ SE, $P \leq 0.05$. (**B**) Representative images of embryos displaying TUNEL or caspase-3 positive cells; $n = 20-30$ embryos in each group. Embryos cultured in 350 mOsm sucrose hyperosmotic medium displayed a greater incidence of apoptotic nuclei than embryos cultured in the control KSOMaa or 300 mOsm groups; scale bar = 20 μM.

nuclei in embryos treated with 350 mOsm sucrose medium when compared with normal KSOMaa or hyperosmotic glycerol medium (Fig. 5A). Comparison of means by independent sample *t*-tests and one-way ANOVA indicated that there was no significant difference in apoptotic cells between KSOMaa controls, 300 mOsm glycerol, 300 mOsm sucrose and 350 mOsm glycerol-treated groups (Fig. 5A). To validate this finding further, we also measured apoptosis using a caspase-3 assay. The caspase-3 assay revealed that embryos treated for 6 h in 350 mOsm sucrose medium also displayed a significant increase in apoptosis ($P \leq 0.05$) when compared with KSOMaa or hyperosmotic glycerol medium. Figure 5B depicts representative images of TUNEL and caspase-3-labeled apoptotic cells in embryos cultured for 6 h in KSOMaa and 350 mOsm KSOMaa sucrose treatments.

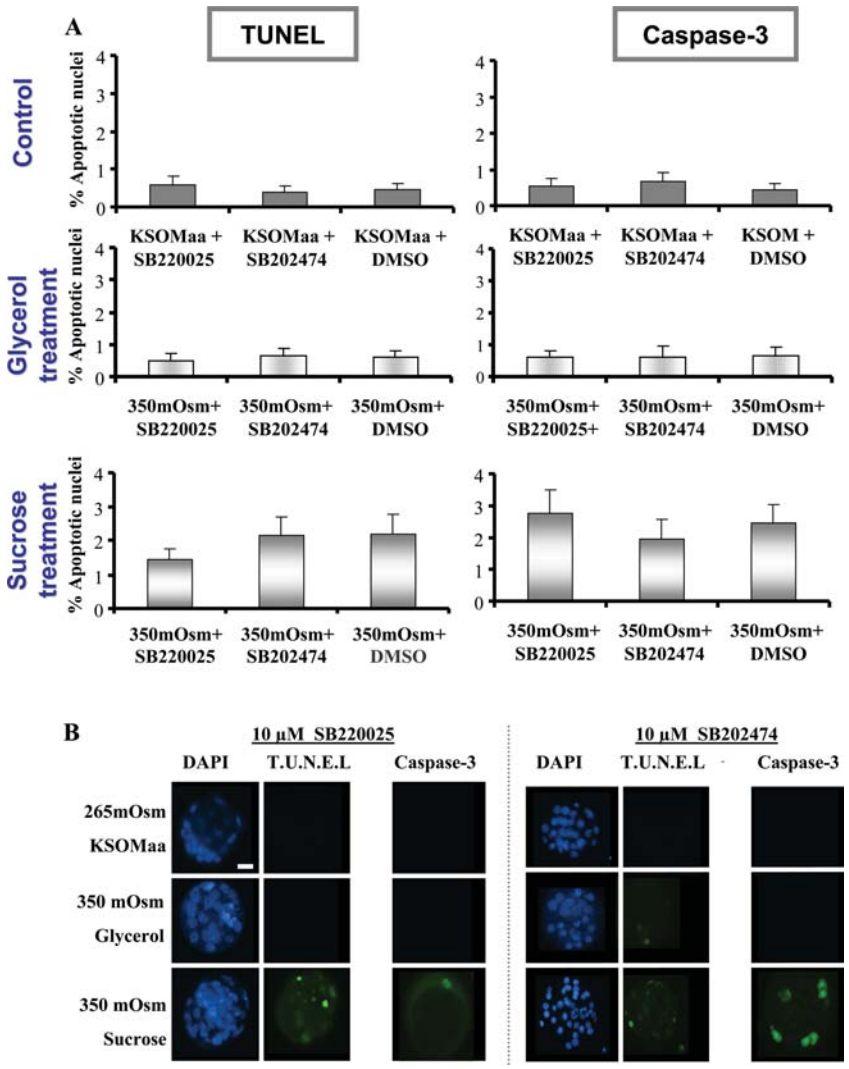

Figure 6 Apoptosis in hyperosmotic media-treated embryos plus MAPK14/11 inhibitor. TUNEL and caspase-3 assays were used to assess apoptosis in blastocysts following exposure of 8-cell stage embryos to hyperosmotic medium treatment for 6 h in the presence of SB220025. Blockade of the MAPK14/11 pathway did not affect the appearance of normal elevated apoptosis levels following exposure to sucrose hyperosmotic media; mean ± SE, $P \leq 0.05$. (**B**) Representative images of TUNEL or caspase-3-treated embryos exposed to 350 mOsm hyperosmotic media (sucrose or glycerol) + SB220025 or 350 mOsm hyperosmotic media (sucrose or glycerol) + SB202474. Embryos cultured in 350 mOsm sucrose hyperosmotic + SB220025 medium displayed a greater incidence of apoptotic nuclei than embryos cultured in the control KSOMaa + SB220025 or 350 mOsm glycerol + SB220025. There was no significant difference in apoptosis levels between embryos cultured in the presence of SB220025 or SB202474; scale bar = 20 μM. $n = 20–30$ embryos in each group.

Apoptosis following culture in KSOMaa and 350 mOsm sucrose or glycerol medium in the presence of MAPK14/11 or MAPK 8 blocker

We next investigated whether inhibition of the MAPK14/11 pathway would affect apoptosis after embryos were cultured in hyperosmotic medium. Figure 6 illustrates that embryos cultured in the 350 mOsm sucrose medium in the presence of the MAPK14/11 inhibitor displayed similar levels of apoptosis using both the TUNEL and caspase-3 assays as did embryos cultured in the MAPK14/11 inactive analog SB202474 and DMSO. Figure 6B depicts representative images of TUNEL and caspase-3-labeled apoptotic cells in embryos cultured for 6 h in KSOMaa, 350 mOsm KSOMaa using glycerol or sucrose treatments in the presence of SB220025. We next characterized whether inhibition of the MAPK8 pathway would affect apoptosis following embryo culture in hyperosmotic medium. Apoptosis was not affected by blocking MAPK8 activity in control (KSOMaa) culture embryos or in embryos cultured in glycerol treatment media (Fig. 7). However, for embryos cultured in the 350 mOsm sucrose treatment medium, blockade of MAPK8 activity resulted in a significant decrease in apoptosis as assessed by both TUNEL and caspase-3 assays ($P \leq 0.05$) (Fig. 7). Figure 7B depicts representative images of TUNEL and caspase-3-labeled apoptotic cells in embryos cultured

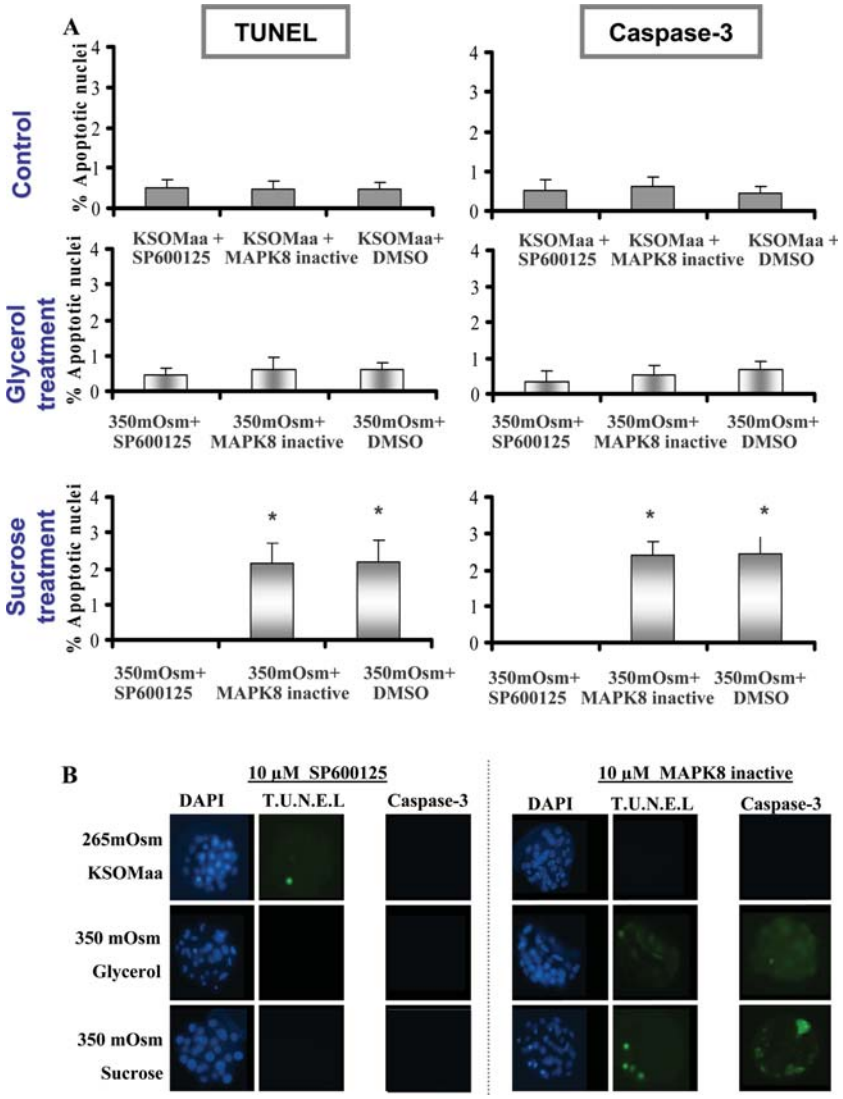

Figure 7 Apoptosis in hyperosmotic media-treated embryos plus MAPK8 inhibitor. (**A**) TUNEL and caspase-3 assays were used to assess apoptosis in blastocysts following exposure of 8-cell stage embryos to hyperosmotic medium treatment for 6 h in the presence of SP600125; mean ± SE, $P \leq 0.05$. MAPK8 pathway inhibition completely blocked apoptosis following treatment with 350 mOsm sucrose hyperosmotic media. (**B**) Representative images of TUNEL or caspase-3-treated embryos exposed to 350 mOsm hyperosmotic media (sucrose or glycerol) + SP600125 or 350 mOsm hyperosmotic media (sucrose or glycerol) + MAPK8 inactive inhibitor. Embryos cultured in 350 mOsm sucrose hyperosmotic + SP600125 medium displayed no incidence of apoptotic nuclei compared with embryos cultured in the control KSOMaa + SP600125 or 350 mOsm glycerol + SP600125. There was a significant difference in apoptosis levels between embryos cultured in the presence 350 mOsm sucrose hyperosmotic + SP600125 and embryos cultured in 350 mOsm sucrose hyperosmotic + MAPK8 inactive inhibitor; scale bar = 20 µM. $n = 20–30$ embryos in each group.

for 6 h in KSOMaa, 300 and 350 mOsm KSOMaa using glycerol or sucrose treatments.

Discussion

In this study, we have demonstrated that preimplantation embryos may be cultured at physiological osmolarities if the culture medium is supplemented with glycerol instead of sucrose. In addition, AQP 3 and 9 gene expression and protein localization are regulated by osmotic treatment, indicating that AQPs are important components of the adaptive mechanisms that preimplantation embryos employ in response to changing environment. Interestingly, *Aqp 3* and *9* mRNA levels and protein distribution were only affected by sucrose treatment and not by glycerol treatment, indicating that AQP 3 and 9 function to alleviate cellular stress imposed by the external environment. This conclusion was validated by our observations that glycerol treatment did not result in elevated apoptosis, unlike the sucrose treatment. Thus, AQP 3 and 9 also participate in regulating apoptosis by reducing cellular stress. Furthermore, we have demonstrated by the use of specific and potent MAPK inhibitors that the regulation of AQP expression and localization primarily occurs by the MAPK14/11 pathway, whereas apoptosis is primarily regulated by the MAPK8

pathway. Taken together, these outcomes support the overall conclusion that AQP 3 and 9 function in part to alleviate cellular osmotic stress and indicate that the MAPK14/11 and MAPK8 pathways are important stress-activated pathways that have distinct roles to play in regulating embryonic responses to stress.

AQPs act as water channels, allowing water and solutes to cross the plasma membrane in the absence of a steep osmotic gradient. Their physiological role has been defined as regulating near iso-osmotic water transport (Ishibashi *et al*., 2000; Agre and Kozono, 2003; Barcroft *et al*., 2003; Agre, 2006). Exposure to hyperosmotic conditions would increase the ionic gradient across the plasma membrane and this may provide a stimulus for enhanced expression of AQPs in an attempt to alleviate the stress. The shift in AQP protein distribution from a primarily cortical to a cytoplasmic distribution may reflect the progression of newly synthesized protein *en route* to the plasma membrane. This finding would be consistent with our prediction that the alterations in AQP expression that occur following exposure to hyperosmotic medium reflect an adaptive cellular response to culture-induced stress.

The MAPK14/11 pathway is activated in response to hyperosmotic treatment in the embryo and in other cell types (Arima *et al*., 2003; Fong *et al*., 2007). In addition, MAPK signaling is implicated in the regulation of AQP 3 and 9 (Arima *et al*., 2003; Cao *et al*., 2006) and other AQPs (Hoffert *et al*., 2000; Umenishi and Schrier, 2003; Hansen and Galtung, 2007). These studies noted, however, that the total protein levels for the MAPK pathway did not increase in response to hyperosmotic stress and that signaling occurred via increased phosphorylation of the MAPK pathway constituents. Our results certainly support the conclusion that the hyperosmotic treatment-induced influences on AQP expression and distribution are primarily regulated by MAPK14/11 in the preimplantation embryo. Of interest, embryos cultured in normal KSOMaa + MAPK14/11 inhibitor did not show any changes in *Aqp 3* and *9* mRNA expression or protein localization. Therefore, MAPK14/11 regulation of AQP 3 and 9 may be primarily directed during responses to hyperosmotic stress and is not a component of the normal regulatory mechanisms controlling basal AQP expression during preimplantation development.

In complete contrast to the results obtained following sucrose hyperosmotic treatment, embryos cultured in 350 mOsm glycerol hyperosmotic medium were morphologically identical to embryos cultured in KSOMaa. As well, they did not demonstrate any changes in mRNA expression or protein localization for *Aqp 9*. We did, however, observe a decrease in the mRNA expression of AQP 3 after 6 and 24 h in embryos treated with hyperosmotic glycerol media. This could be indicative of the embryo attempting to regulate the accumulation of glycerol within the blastomeres by decreasing the expression of an aquaglyceroporin such as AQP 3. This result would indicate that *Aqp 3* mRNA is responsive but *Aqp 9* mRNA is not, demonstrating that these AQPs are differentially regulated and can respond independently to environmental changes that the embryo experiences. Offenberg *et al*. (2005) examined the expression of *Aqp 3* and *Aqp 9* in blastocysts cultured from the 8-cell compacted embryo in hyperosmotic conditions for 40 h and did not report any changes in mRNA levels. Our studies examined effects over a much shorter time period (3, 6 and 24 h). We predict that our results and those of Offenberg *et al*. (2005) suggest that the influences on AQP expression occur fairly rapidly following exposure to hyperosmotic medium and then may return to basal levels by 40 h after exposure to hyperosmotic medium. Offenberg *et al*. (2005) did, however, show increases in *Aqp 3* and *9* mRNA expression after blastocyst puncture, which supports our observation that AQP 3 and 9 expression is regulated under stressful conditions.

The ability of treated embryos to progress in normal numbers to the blastocyst stage in the 350 mOsm glycerol medium is intriguing. We would propose that this occurrence is due in part to the presence of AQP 3 and 9 and their role as aquaglyceroporins to promote the movement of glycerol into the cell down the glycerol concentration gradient (Zelenina *et al*., 2004; Hara-Chikuma and Verkman, 2005; Karlgren *et al*., 2005; Hara-Chikuma and Verkman, 2006; Liu *et al*., 2007; Rojek *et al*., 2007). The presence of AQP 3 and 9 could alleviate the osmotic gradient, establishing equilibrium with the external medium and thus eliminating the presence of osmotic stress on the embryo in the 350 mOsm glycerol medium. Barcroft *et al*. (2003) demonstrated that AQPs were present and functional in the preimplantation embryo by exposing blastocysts to an 1800 mOsm glycerol solution. Under these conditions, the blastocysts initially collapse but then recover completely within 3 min to restore their original shape and volume (Barcroft *et al*., 2003). In this example, normal expression of aquaglyceroporins allowed the embryos to transport glycerol across the blastocyst membrane quickly and restore normal blastocyst volume, however, when the same experiment was conducted using sucrose instead of glycerol, embryos were not able to regain their expanded form (Barcroft *et al*., 2003). In conclusion, our outcomes would suggest that culture in 350 mOsm glycerol medium does not impair development to the blastocyst stage *in vitro*, does not activate the MAPK14/11 pathway or alter AQP expression, thus it does not appear to evoke a cellular stress response.

Apoptosis is an important mechanism linked to the cellular response to stress (Kurzawa *et al*., 2002; Esfandiari *et al*., 2005; Zander *et al*., 2006; Esfandiari *et al*., 2007; Oh *et al*., 2007; Xie *et al*., 2007). Apoptotic mechanisms are well defined during preimplantation development, and this developmental event is normally first observed at the blastocyst stage (Pierce *et al*., 1989; Hardy, 1997, 1999; Warner *et al*., 1998; Byrne *et al*., 1999; Huppertz *et al*., 1999; Pampfer, 2000; Levy *et al*., 2001). Both MAPK14/11 and MAPK8 pathways mediate cellular apoptosis and it is for this reason that we investigated the effects of exposure to hyperosmotic medium treatment on apoptosis. Our results indicate that hyperosmotic stress using sucrose treatment will increase the levels of apoptosis. However, 350 mOsm glycerol medium does not elicit a similar apoptotic response. Xie *et al*. (2007) demonstrated that the MAPK8 pathway regulates apoptosis during preimplantation development. Interestingly, our results support those of Xie *et al*. (2007) and suggest that the MAPK8 pathway is the primary mediator of osmotic stress-induced apoptosis. Our outcomes support our assertion that the exposure to glycerol hyperosmotic medium does not elicit a cellular stress response due to the action of AQP 3 and 9, which alleviate the osmotic stress by allowing glycerol to cross the cell membrane. Thus, AQP 3 and 9 may also function to regulate the occurrence of apoptosis in cell systems. Clearly, blockade of the MAPK14/11 pathway had no effect on hyperosmotic treatment-induced apoptosis, whereas blockade of the MAPK8 pathway completely negated the increased apoptosis observed following treatment with hyperosmotic sucrose medium. Treatment with

either the MAPK14/11 or MAPK8 inhibitor applied to normal KSOMaa media control embryos had no effect on reducing embryonic apoptotic levels, indicating that basal apoptotic levels are unlikely to be under the control of either pathway. Thus, our experiments have also shed light on the roles of two MAPK pathways, MAPK14/11 and MAPK8 in regulating apoptosis, and also their roles in response to embryonic exposure to hyperosmotic treatment. Each pathway has a distinct but important contribution to the mechanisms controlling preimplantation development.

We therefore conclude that the changes in *Aqp 3* and *9* mRNA levels and protein distribution are the components of a rapid adaptive response that the embryo employs to alleviate cellular stress. The sucrose treatment exceeds the adaptive capacity of the preimplantation embryo, resulting in the activation of apoptosis and induced cell death. MAPK14/11 activation is therefore, in this context, a component of the rapid adaptive stress response mechanism, whereas the MAPK8 pathway regulates apoptosis. Our results indicate that culture in 350 mOsm KSOMaa + glycerol medium is not detrimental for preimplantation development and this may allow early embryo culture at more physiological osmolarities. These outcomes improve our understanding of the embryonic adaptive mechanisms to environmental stress and indicate that AQPs are critical components of the embryo's response to stressful environments. They may also lead to further developments in the optimization of culture media for the production of mammalian preimplantation embryos *in vitro*.

Acknowledgements

Our gratitude is extended to Dr Michele Calder and Holly Giannatselis for their expertise and assistance with embryo collections, and also to Dr Michele Calder and Robert A. Bell for editorial contributions.

Funding

This research was supported by an operating grant from the Canadian Institutes of Health Research (CIHR) to A.J.W. C.E.B. is supported by a Department of Obstetrics and Gynaecology Graduate Scholarship from the University of Western Ontario.

References

Agre P. The aquaporin water channels. *Proc Am Thorac Soc* 2006;**3**:5–13.

Agre P, Kozono D. Aquaporin water channels: molecular mechanisms for human diseases. *FEBS Lett* 2003;**555**:72–78.

Arima H, Yamamoto N, Sobue K, Umenishi F, Tada T, Katsuya H, Asai K. Hyperosmolar mannitol simulates expression of aquaporins 4 and 9 through a p38 mitogen-activated protein kinase-dependent pathway in rat astrocytes. *J Biol Chem* 2003;**278**:44525–44534.

Barcroft LC, Offenberg H, Thomsen P, Watson AJ. Aquaporin proteins in murine trophectoderm mediate transepithelial water movements during cavitation. *Dev Biol* 2003;**256**:342–354.

Barcroft LC, Moseley AE, Lingrel JB, Watson AJ. Deletion of the Na/K-ATPase alpha1-subunit gene (Atp1a1) does not prevent cavitation of the preimplantation mouse embryo. *Mech Dev* 2004;**121**:417–426.

Betts DH, Barcroft LC, Watson AJ. Na/K-ATPase-mediated 86Rb+ uptake and asymmetrical trophectoderm localization of alpha1 and alpha3 Na/K-ATPase isoforms during bovine preattachment development. *Dev Biol* 1998;**197**:77–92.

Bogdarina I, Welham S, King PJ, Burns SP, Clark AJ. Epigenetic modification of the renin-angiotensin system in the fetal programming of hypertension. *Circ Res* 2007;**100**:520–526.

Byrne AT, Southgate J, Brison DR, Leese HJ. Analysis of apoptosis in the preimplantation bovine embryo using TUNEL. *J Reprod Fertil* 1999; **117**:97–105.

Cao C, Sun Y, Healey S, Bi Z, Hu G, Wan S, Kouttab N, Chu W, Wan Y. EGFR-mediated expression of aquaporin-3 is involved in human skin fibroblast migration. *Biochem J* 2006;**400**:225–234.

Collins JL, Baltz JM. Estimates of mouse oviductal fluid tonicity based on osmotic responses of embryos. *Biol Reprod* 1999;**60**:1188–1193.

Diamond MP, Pettway ZY, Logan J, Moley K, Vaughn W, DeCherney AH. Dose–response effects of glucose, insulin, and glucagon on mouse pre-embryo development. *Metabolism* 1991;**40**:566–570.

Ecelbarger CA, Terris J, Frindt G, Echevarria M, Marples D, Nielsen S, Knepper MA. Aquaporin-3 water channel localization and regulation in rat kidney. *Am J Physiol* 1995;**269**:F663–F672.

Echevarria M, Windhager EE, Frindt G. Selectivity of the renal collecting duct water channel aquaporin-3. *J Biol Chem* 1996;**271**:25079–25082.

Esfandiari N, Falcone T, Agarwal A, Attaran M, Nelson DR, Sharma RK. Protein supplementation and the incidence of apoptosis and oxidative stress in mouse embryos. *Obstet Gynecol* 2005;**105**:653–660.

Esfandiari N, Falcone T, Goldberg JM, Agarwal A, Sharma RK. Heat-shock proteins modulate the incidence of apoptosis and oxidative stress in preimplantation mouse embryos. *Fertil Steril* 2007;**87**:1214–1217.

Fong B, Watson PH, Watson AJ. Mouse preimplantation embryo responses to culture medium osmolarity include increased expression of CCM2 and p38 MAPK activation. *BMC Dev Biol* 2007;**7**:2.

Gardner DK, Leese HJ. Concentrations of nutrients in mouse oviduct fluid and their effects on embryo development and metabolism *in vitro*. *J Reprod Fertil* 1990;**88**:361–368.

Hansen AK, Galtung HK. Aquaporin expression and cell volume regulation in the SV40 immortalized rat submandibular acinar cell line. *Pflugers Arch* 2007;**453**:787–796.

Hara-Chikuma M, Verkman AS. Aquaporin-3 functions as a glycerol transporter in mammalian skin. *Biol Cell* 2005;**97**:479–486.

Hara-Chikuma M, Verkman AS. Physiological roles of glycerol-transporting aquaporins: the aquaglyceroporins. *Cell Mol Life Sci* 2006; **63**:1386–1392.

Hara-Chikuma M, Verkman AS. Aquaporin-3 facilitates epidermal cell migration and proliferation during wound healing. *J Mol Med* 2008; **86**:221–231.

Hardy K. Cell death in the mammalian blastocyst. *Mol Hum Reprod* 1997; **3**:919–925.

Hardy K. Apoptosis in the human embryo. *Rev Reprod* 1999;**4**:125–134.

Hickson JA, Fong B, Watson PH, Watson AJ. PP2Cdelta (Ppm1d, WIP1), an endogenous inhibitor of p38 MAPK, is regulated along with Trp53 and Cdkn2a following p38 MAPK inhibition during mouse preimplantation development. *Mol Reprod Dev* 2007;**74**: 821–834.

Hoffert JD, Leitch V, Agre P, King LS. Hypertonic induction of aquaporin-5 expression through an ERK-dependent pathway. *J Biol Chem* 2000; **275**:9070–9077.

Huerta S, Goulet EJ, Huerta-Yepez S, Livingston EH. Screening and detection of apoptosis. *J Surg Res* 2007;**139**:143–156.

Huppertz B, Frank HG, Kaufmann P. The apoptosis cascade—morphological and immunohistochemical methods for its visualization. *Anat Embryol (Berl)* 1999;**200**:1–18.

Ishibashi K, Sasaki S, Fushimi K, Uchida S, Kuwahara M, Saito H, Furukawa T, Nakajima K, Yamaguchi Y, Gojobori T. Molecular cloning and expression of a member of the aquaporin family with permeability to glycerol and urea in addition to water expressed at

the basolateral membrane of kidney collecting duct cells. *Proc Natl Acad Sci USA* 1994;**91**:6269–6273.

Ishibashi K, Sasaki S, Fushimi K, Yamamoto T, Kuwahara M, Marumo F. Immunolocalization and effect of dehydration on AQP3, a basolateral water channel of kidney collecting ducts. *Am J Physiol* 1997; **272**:F235–F241.

Ishibashi K, Kuwahara M, Gu Y, Tanaka Y, Marumo F, Sasaki S. Cloning and functional expression of a new aquaporin (AQP9) abundantly expressed in the peripheral leukocytes permeable to water and urea, but not to glycerol. *Biochem Biophys Res Commun* 1998; **244**:268–274.

Ishibashi K, Kuwahara M, Sasaki S. Molecular biology of aquaporins. *Rev Physiol Biochem Pharmacol* 2000;**141**:1–32.

Jones DH, Davies TC, Kidder GM. Embryonic expression of the putative gamma subunit of the sodium pump is required for acquisition of fluid transport capacity during mouse blastocyst development. *J Cell Biol* 1997;**139**:1545–1552.

Karlgren S, Pettersson N, Nordlander B, Mathai JC, Brodsky JL, Zeidel ML, Bill RM, Hohmann S. Conditional osmotic stress in yeast: a system to study transport through aquaglyceroporins and osmostress signaling. *J Biol Chem* 2005;**280**:7186–7193.

Koyama Y, Yamamoto T, Kondo D, Funaki H, Yaoita E, Kawasaki K, Sato N, Hatakeyama K, Kihara I. Molecular cloning of a new aquaporin from rat pancreas and liver. *J Biol Chem* 1997; **272**:30329–30333.

Kurzawa R, Glabowski W, Baczkowski T, Brelik P. Evaluation of mouse preimplantation embryos exposed to oxidative stress cultured with insulin-like growth factor I and II, epidermal growth factor, insulin, transferrin and selenium. *Reprod Biol* 2002;**2**:143–162.

Kwong WY, Wild AE, Roberts P, Willis AC, Fleming TP. Maternal undernutrition during the preimplantation period of rat development causes blastocyst abnormalities and programming of postnatal hypertension. *Development* 2000;**127**:4195–4202.

Leese HJ, Donnay I, Thompson JG. Human assisted conception: a cautionary tale. Lessons from domestic animals. *Hum Reprod* 1998; **13**(Suppl. 4):184–202.

Levy RR, Cordonier H, Czyba JC, Guerin JF. Apoptosis in preimplantation mammalian embryo and genetics. *Ital J Anat Embryol* 2001; **106**:101–108.

Li X, Kato Y, Tsunoda Y. Comparative analysis of development-related gene expression in mouse preimplantation embryos with different developmental potential. *Mol Reprod Dev* 2005;**72**:152–160.

Liu Y, Promeneur D, Rojek A, Kumar N, Frokiaer J, Nielsen S, King LS, Agre P, Carbrey JM. Aquaporin 9 is the major pathway for glycerol uptake by mouse erythrocytes, with implications for malarial virulence. *Proc Natl Acad Sci USA* 2007;**104**:12560–12564.

Ma T, Frigeri A, Hasegawa H, Verkman AS. Cloning of a water channel homolog expressed in brain meningeal cells and kidney collecting duct that functions as a stilbene-sensitive glycerol transporter. *J Biol Chem* 1994;**269**:21845–21849.

MacPhee DJ, Jones DH, Barr KJ, Betts DH, Watson AJ, Kidder GM. Differential involvement of Na(+),K(+)-ATPase isozymes in preimplantation development of the mouse. *Dev Biol* 2000; **222**:486–498.

Madan P, Rose K, Watson AJ. Na/K-ATPase beta1 subunit expression is required for blastocyst formation and normal assembly of trophectoderm tight junction-associated proteins. *J Biol Chem* 2007; **282**:12127–12134.

Natale DR, Paliga AJ, Beier F, D'souza SJ, Watson AJ. p38 MAPK signaling during murine preimplantation development. *Dev Biol* 2004;**268**:76–88.

Offenberg H, Barcroft LC, Caveney A, Viuff D, Thomsen PD, Watson AJ. mRNAs encoding aquaporins are present during murine preimplantation development. *Mol Reprod Dev* 2000;**57**:323–330.

Offenberg H, Thomsen PD. Functional challenge affects aquaporin mRNA abundance in mouse blastocysts. *Mol Reprod Dev* 2005;**71**:422–430.

Oh SJ, Gong SP, Lee ST, Lee EJ, Lim JM. Light intensity and wavelength during embryo manipulation are important factors for maintaining viability of preimplantation embryos *in vitro*. *Fertil Steril* 2007;**88**:1150–1157.

Paliga AJ, Natale DR, Watson AJ. p38 mitogen-activated protein kinase (MAPK) first regulates filamentous actin at the 8–16-cell stage during preimplantation development. *Biol Cell* 2005;**97**:629–640.

Pampfer S. Apoptosis in rodent peri-implantation embryos: differential susceptibility of inner cell mass and trophectoderm cell lineages—a review. *Placenta* 2000;**21**(Suppl. A):S3–S10.

Pierce GB, Lewellyn AL, Parchment RE. Mechanism of programmed cell death in the blastocyst. *Proc Natl Acad Sci USA* 1989;**86**:3654–3658.

Rivard CJ, Almeida NE, Berl T, Capasso JM. The gamma subunit of Na/K-ATPase: an exceptional, small transmembrane protein. *Front Biosci* 2005;**10**:2604–2610.

Rojek AM, Skowronski MT, Fuchtbauer EM, Fuchtbauer AC, Fenton RA, Agre P, Frokiaer J, Nielsen S. Defective glycerol metabolism in aquaporin 9 (AQP9) knockout mice. *Proc Natl Acad Sci USA* 2007; **104**:3609–3614.

Saraste A, Pulkki K. Morphologic and biochemical hallmarks of apoptosis. *Cardiovasc Res* 2000;**45**:528–537.

Steeves CL, Baltz JM. Regulation of intracellular glycine as an organic osmolyte in early preimplantation mouse embryos. *J Cell Physiol* 2005; **204**:273–279.

Steeves CL, Hammer MA, Walker GB, Rae D, Stewart NA, Baltz JM. The glycine neurotransmitter transporter GLYT1 is an organic osmolyte transporter regulating cell volume in cleavage-stage embryos. *Proc Natl Acad Sci USA* 2003;**100**:13982–13987.

Umenishi F, Schrier RW. Hypertonicity-induced aquaporin-1 (AQP1) expression is mediated by the activation of MAPK pathways and hypertonicity-responsive element in the AQP1 gene. *J Biol Chem* 2003;**278**:15765–15770.

Warner CM, Exley GE, McElhinny AS, Tang C. Genetic regulation of preimplantation mouse embryo survival. *J Exp Zool* 1998;**282**:272–279.

Xie Y, Puscheck EE, Rappolee DA. Effects of SAPK/JNK inhibitors on preimplantation mouse embryo development are influenced greatly by the amount of stress induced by the media. *Mol Hum Reprod* 2006; **12**:217–224.

Xie Y, Zhong W, Wang Y, Trostinskaia A, Wang F, Puscheck EE, Rappolee DA. Using hyperosmolar stress to measure biologic and stress-activated protein kinase responses in preimplantation embryos. *Mol Hum Reprod* 2007;**13**:473–481.

Zander DL, Thompson JG, Lane M. Perturbations in mouse embryo development and viability caused by ammonium are more severe after exposure at the cleavage stages. *Biol Reprod* 2006;**74**:288–294.

Zelenina M, Tritto S, Bondar AA, Zelenin S, Aperia A. Copper inhibits the water and glycerol permeability of aquaporin-3. *J Biol Chem* 2004; **279**:51939–51943.

Submitted on June 18, 2008; resubmitted on December 19, 2008; accepted on January 7, 2009